ANALYSIS OF LMFBR CONTAINMENT RESPONSE TO AN HCDA USING A MULTIFIELD EULERIAN CODE

MASTER

CONF-770807--52

H. Y. Chu and Y. W. Chang

Prepared for

4th SMIRT Conference
San Francisco, CA
August 15-19, 1977

ARGONNE NATIONAL LABORATORY, ARGONNE, ILLINOIS

operated under contract W-31-109-Eng-38 for the
U. S. ENERGY RESEARCH AND DEVELOPMENT ADMINISTRATION

ANALYSIS OF LMFBR CONTAINMENT RESPONSE TO AN HCDA USING A MULTIFIELD EULERIAN CODE

H. Y. Chu and Y. W. Chang
Reactor Analysis and Safety Division
Argonne National Laboratory
Argonne, Illinois 60439, U. S. A.

1. Introduction

There are many different types of materials in a primary system. Each material may exist in several phases. During a hypothetical core disruptive accident (HCDA), a core meltdown may cause the fuel cladding to rupture and the fuel fragments to penetrate into the sodium coolant. The heat in the molten fuel may cause the liquid sodium to boil, changing its phase. The interactions between materials are so complicated that a single-material model with homogenized material properties is not adequate. In order to analyze the above phenomena more realistically, a Multifield Implicit Contineous-fluid Eulerian containment code (MICE) is being developed at Argonne National Laboratory (ANL) to solve the multifield fluid-flow problems in which the interpenetrations of materials, heat transfer, and phase changes are considered in the analysis.

The hydrodynamics of the MICE code is based upon the implicit multifield (IMF) method developed by Harlow and Amsden [1,2]. A partial donor-cell formulation is used for the calculation of the convective fluxes to minimize the truncation errors, while the Newton-Raphson method is used for the numerical iterations. An implicit treatment of the mass convection together with the equation of state for each material enables the method to be applicable to both compressible and incompressible flows. A partial implicit treatment of the momentum-exchange functions allows the coupling drag forces between two material fields to range from very weak to those strong enough to tie the fields completely.

The differential equations and exchange functions used in the MICE code, and the treatment of the fluid and structure interactions as well as the numerical procedure are described in Sect. 2. Section 3 gives two sample calculations to illustrate the present capability of the MICE code.

2. Description of the Implicit Eulerian Method for Solving Multifield Fluid-flow Problems

2.1 Differential Equations

As mentioned earlier, a primary containment system contains many different types of materials. Each material may exist in several phases. The term "field" used here is to distinguish one phase of a material from the other phases of the same material and all the phases of the other material. For example, sodium vapor is considered as one field; liquid sodium and inert gas are considered to be other fields. Each field is governed by the following conservative equations:

$$\frac{\partial \rho'}{\partial t} + \nabla\cdot(\rho' u) = S_\rho , \tag{1}$$

$$\frac{\partial (\rho' u)}{\partial t} + \nabla\cdot(\rho' uu) = S_m - \theta\nabla p + V + \rho' g + K(\bar{u}-u), \tag{2}$$

and

$$\frac{\partial (\rho' I)}{\partial t} + \nabla\cdot(u\rho' I) = \frac{\theta p}{\rho}\left[\frac{\partial \rho}{\partial t} + u\cdot\nabla\rho\right] + S_i + R(\bar{T}-T) + \Lambda + V_i + \nabla\cdot(\kappa\theta\nabla T), \tag{3}$$

where ρ' is the macroscopic material density; u a velocity vector with two components in radial and axial directions, respectively; S_p, S_m and S_i the respective sources (or sinks) for the mass, momentum, and energy terms due to phase transition, chemical process, and similar effects; p the pressure; V the momentum-density source from viscous effects; g the acceleration of gravity; K the drag function; $\bar{u}$ the resistive velocity; I the internal energy; ρ the microscopic material density; R the energy exchange function; $\bar{T}$ the mean exchange temperature; T the temperature; Λ the rate of energy generated by exchange of momentum; V_i the energy density from viscous dissipation; κ the heat-conduction coefficient.

Subscripts are used to identify the fluid variables for a particular field. For example, the volume fraction for field m is represented by θ_m. In any region, we have

$$\sum_m \theta_m = 1 \ . \tag{4}$$

The equation of state for each field can be described by its macroscopic properties such as

$$p_m = f_m(\rho_m, I_m) \ , \tag{5}$$

in which

$$\rho_m = \frac{\rho'_m}{\theta_m} \ . \tag{6}$$

2.2 Exchange Functions

As shown in Eqs. 1-3, the hydrodynamics equations couple one field to the other fields through several exchange functions. These exchange functions are briefly described as follows.

First, consider the interchange due to phase transitions. The change of phase affects all three conservative quantities as indicated by various S terms in Eqs. 1-3. For a single-component material, such as pure water droplets mixed with pure steam, the rate of mass change caused by evaporation and condensation depends on the temperature, pressure, and the sizes of the water droplets and steam bubbles at which the exchange takes place. For multicomponent materials, the rate of mass change also depends crucially on volume fractions. The interchanges of momentum and energy are proportional to the mass changes. Latent heat and momentum mixing should also be included in the energy calculations.

The second interchange is that of momentum. The drag representing momentum exchange for a particular field affected by other fields is usually approximated in terms of binary interactions to avoid complexity. The expressions for the drag and the combination of the drag and resistive velocity are

$$K_m = \sum_n K_{mn} \tag{7}$$

and

$$K_m \bar{u}_m = \sum_n K_{mn} u_n \ , \tag{8}$$

where the drag K_{mn} used in the MICE code is of the form [1]

$$K_{mn} = \frac{3}{2}\theta_m\theta_n\left(\frac{1}{r_m}+\frac{1}{r_n}\right)^2\left[\frac{3\mu_m\mu_n}{\mu_m+\mu_n} + \frac{C_D\rho_m\rho_n|u_m-u_n|r_m r_n}{4(r_m\rho_n+r_n\rho_m)}\right], \tag{9}$$

in which r represents the size scale and C_D is a coefficient of approximately unit magnitude. The viscosity μ depends on the temperature, critical pressure, molecular weight, etc.

Another exchange function, which represents the heat energy transferred per unit volume per unit time, can be also expressed by the binary process as

$$R_m = \sum_n R_{mn} \tag{10}$$

and

$$R_m \bar{T}_m = \sum_n R_{mn} T_n \tag{11}$$

Transfers of this type of energy depends on many factors such as contact area and temperature difference. The detail of this process is very complicated, especially as it involves relative motions. More extensive discussions concerning the exchange functions are given by Soo [3], Kalinin [4], and others.

2.3 Fluid-structure Interactions

A nonlinear finite-element scheme with convected coordinates given by Belytschko and Hsieh [5] is adopted for the MICE code to analyze the structural responses due to fluid-structure interactions. The method solves large-displacement and small-strain problems with material nonlinearities.

At present, the only type of structural element considered for MICE analysis is the conical shell element with two nodal points. The masses at each node are lumped in such a way that the translational and rotational inertias are equivalent to the mass and mass moment, respectively, of the segment between the node and the midpoint of the element. Inertia due to rotation of the cross section is neglected. Nonlinearities in material are described by multilinear stress-strain relations.

Each element is associated with a convected-coordinate system. The convected coordinates rotate but do not deform with the elements. Rigid-body rotation of the convected coordinate is represented by the rotation of the line connecting two nodes of the element. Flexibilities of the element are described by the transverse- and axial-displacement shape functions.

Large displacements are counted entirely by the transformation between the global and convected-element coordinates. Within the convected coordinates, the deformation displacements are linearly related to the strains and the nodal forces are linearly related to the stresses.

The fluid and structure calculations are coupled together in such a way that the fluid supplies the structure with a pressure loading which causes motion of the shell element. In return, the shell element imparts motion to the fluid. We require as a boundary condition that the velocity of the fluid normal to the shell element equal to the velocity of that element.

Each shell element has two sets of fluid-cell indices which identify the location of

that element. The shell element is subjected to pressure loading either on both sides or one side only, depending on the element location.

Because explicit time integration is used for the structural part, the time step used in the numerical integration is limited by the longitudal and flexural wave velocities and by the lengths of the elements. For the coupled fluid-structure problems, the integration time step used in the implicit method for the fluid calculation is much larger. This requires that structural calculations involve several time steps in order to coincide with one time step of the fluid calculations.

2.4 Numerical Procedure

The MICE code solves the multifield fluid flow by use of the finite-difference approach. The flow region is subdivided into an Eulerian mesh with rectangular cells. Field variables such as pressure, density, and internal energy are defined in the center of the cell, while velocity components are defined at the cell edges. Partial donor-cell form is used for the convective-flux approximation.

The mass, momentum, and state equations are expressed in implicit forms; their solutions must be obtained by iteration. The numerical calculations for each iteration are performed in two parts. In the first part, the material field in each cell are treated independently. In the second part, a pressure equilibrium is performed among all fields in each cell. The procedure for one time-step calculation is briefly described below.

(1) Calculate viscous and source terms which do not contain advanced-time factors, using field variables from the previous cycle or the specification of the initial conditions.

(2) Calculate D functions (that is the discrepancies of the mass transport equation), which in turn are used in a Newton-Raphson formula to determine the pressure increments for each field.

(3) Calculate densities for each field, using the updated pressures.

(4) Perform an equilibrated pressure in each cell among all material fields, using updated densities. Volume fractions are also simultaneously adjusted at this step.

(5) Calculate velocity components, using the equilibrated pressure. For those cells containing a structural segment, the velocity components are determined in such a way that

$$(V_p - V_b) \cdot n = 0, \tag{12}$$

where V_p is the velocity vector of the field particle at the segment midpoint, V_b is the velocity vector of the segment midpoint given by structural analysis, and n is the unit vector normal to the segment.

(6) Calculate drag functions, using the updated velocities and volume fractions.

Repeat steps 2-6 until the D functions for each field in each cell are sufficiently small, at which stage the iteration is considered to have converged.

(7) Calculate internal energies, using the most updated field varibles.

(8) Calculate structural responses, using corresponding fluid pressures.

3. Sample Problems

The MICE code has been applied to a variety of problems, two of which are described and illustrated here.

3.1 Responses of Reactor-containment System with Internal Obstacles

A reactor initial configuration with the core barrel and core-support structure modelled as rigid obstacles is shown in Fig. 1 (obstacle cells are indicated by a diagonal line). The opening on the core-support structure simulates a perforated plate which provides a passage for the fluids to enter the lower reactor plenum.

It is assumed that there are two types of material in the reactor-containment system. A field-1 type of material (shown by triangles), such as molten fuel, steel, and liquid sodium which has a high sonic velocity, is nearly incompressible and field-2 type of material (represented by dots) such as fuel vapor, sodium vapor, and inert gas, is highly compressible. The initial distribution of the two types of material are approximately proportioned by their marker particles.

After the initiation of a core-disassembly accident, the core region is heated and under high pressure, while the other regions are relatively cool and under ambient pressure. At the beginning of the excursion, the field-2 type of material moves much faster than the field-1 type of material (see velocity-vector plots in Fig. 2). The velocity differences will gradually disappear as the field-1 type of material gains momentum. Core expansion and marker-particle movements at two other instants -- 4.35 ms and 14.35 ms after the start of computation--are shown in Fig. 3. The changes of relative positions between fields indicates an interpenetration of the fields.

3.2 Response of Reactor-containment System with Fluid-structure Interactions

This example deals with the fluid-structure interactions in a reactor-containment system after the initiation of a core-disassembly accident. Again two types of material are considered in the system except that marker particles for the field-1 type of material are represented by diamonds (see Fig. 4). The reactor wall shown along the right side of the computing mesh is approximated by a deformable material which has the following mechanical properties: elastic modulus, 1.998×10^{12} dynes/cm^2; yield stress, 4.315×10^9 dynes/cm^2; plastic modulus, 4.019×10^9 dynes/cm^2; ultimate stress, 4.658×10^9 dynes/cm^2; Poisson's ratio, 0.3. The left side of the computing mesh is bounded by a cylindrical symmetry axis, and the top and bottom sides are considered as rigid free-slip walls. As shown by the marker particles in Fig. 4, the core region contains more highly compressible materials (dots), and the ambient region contains more nearly incompressible materials (diamonds). The core region is initially heated and under a 300-bar pressure. As the coolant being pushed by the core materials moves outward, the reactor wall undergoes an elastic-plastic deformation. The deformations of the reactor wall at two instants -- 3.10 ms and 5.60 ms after the start of computation -- are shown in Fig. 5. The interpenetrations of the two fields of material and core expansions can also be seen for these two configurations.

4. Future Application

The development of the MICE code is continuing. The methodology used by the MICE code involves not only the mechanical properties for each individual field of material, but also the complicated interactions between them. A great deal of research remains to be done in those topics of studies. At this stage of development, MICE code is still limited to a certain number of physical phenomena that will be required for future application.

As can be seen the potential application of MICE code is not limited to the primary containment system, it can also apply to some other reactor system such as cavitating flow in HTS (heat transport system).

5. Acknowledgments

The authors would like to thank Dr. S. H. Fistedis for his encouragement and valuable discussions.

The work described in this paper was performed under the Engineering Mechanics Program of the Reactor Analysis and Safety Division at Argonne National Laboratory which is supported by the Energy Research and Development Administration, U. S. A.

References

[1] HARLOW, F. H., AMSDEN, A. A., "Flow of Interpenetrating Material Phases," J. Comp. Phys. 18, p. 440 (1975).

[2] HARLOW, F. H., AMSDEN, A. A., "Numerical Calculation of Multiphase Fluid Flow," J. Comp. Phys. 17, p. 19 (1975).

[3] SOO, S. L., "Fluid Dynamics of Multiphase Systems," Blaisdell, Waltham, MA, (1967).

[4] KALININ, A. V., "Derivation of Fluid-Mechanics Equations for a Two-Phase Medium with Phase Changes," Heat Transfer-Soviet Research 2, p. 83, May (1970).

[5] BELYTSCHKO, T., HSIEH, B. J., "Non-linear Transient Finite Element Analysis with Convected Coordinates," Int. J. Numerical Method in Engr. 7, p. 255 (1973).

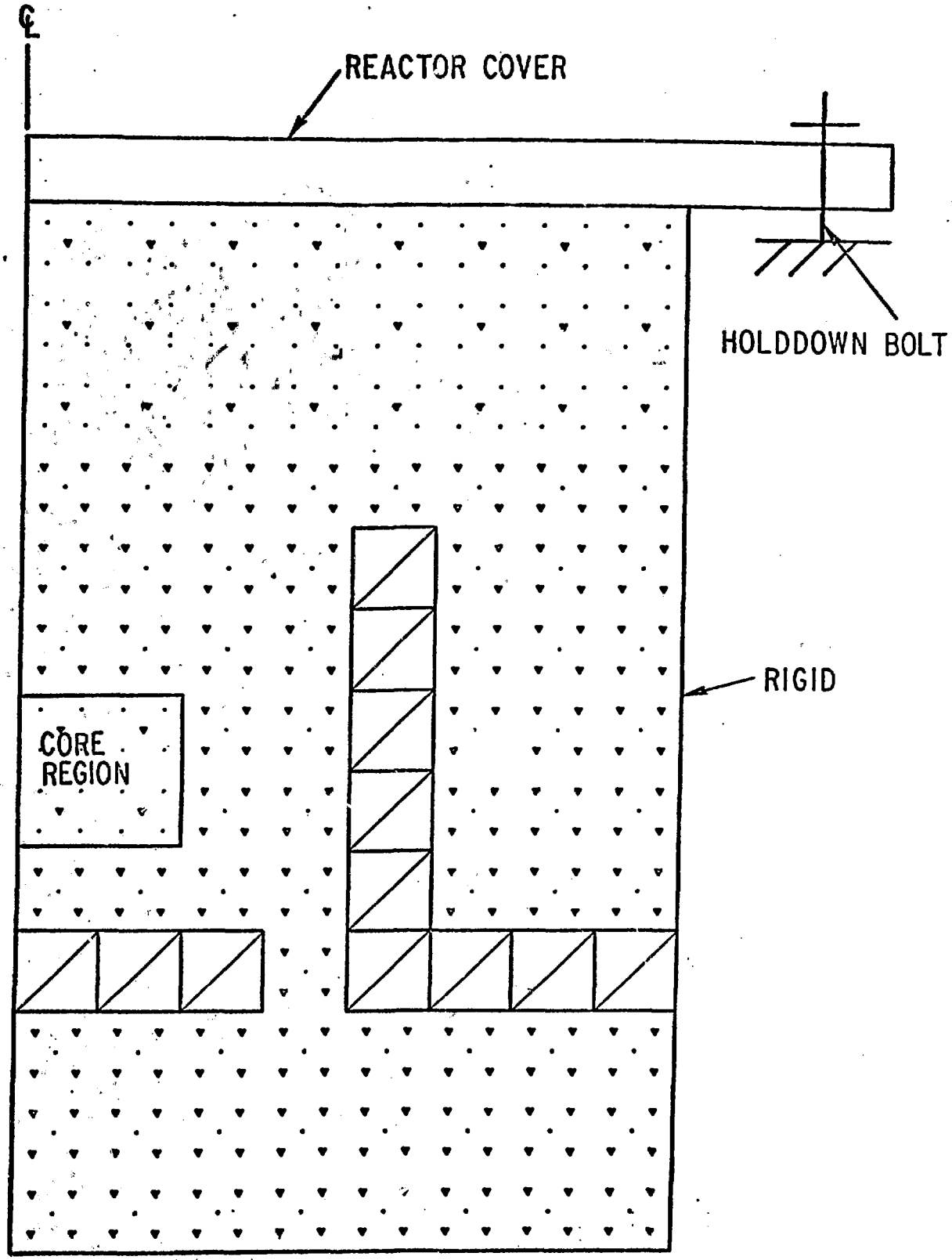

Fig. 1. Initial Configuration (Example 1)

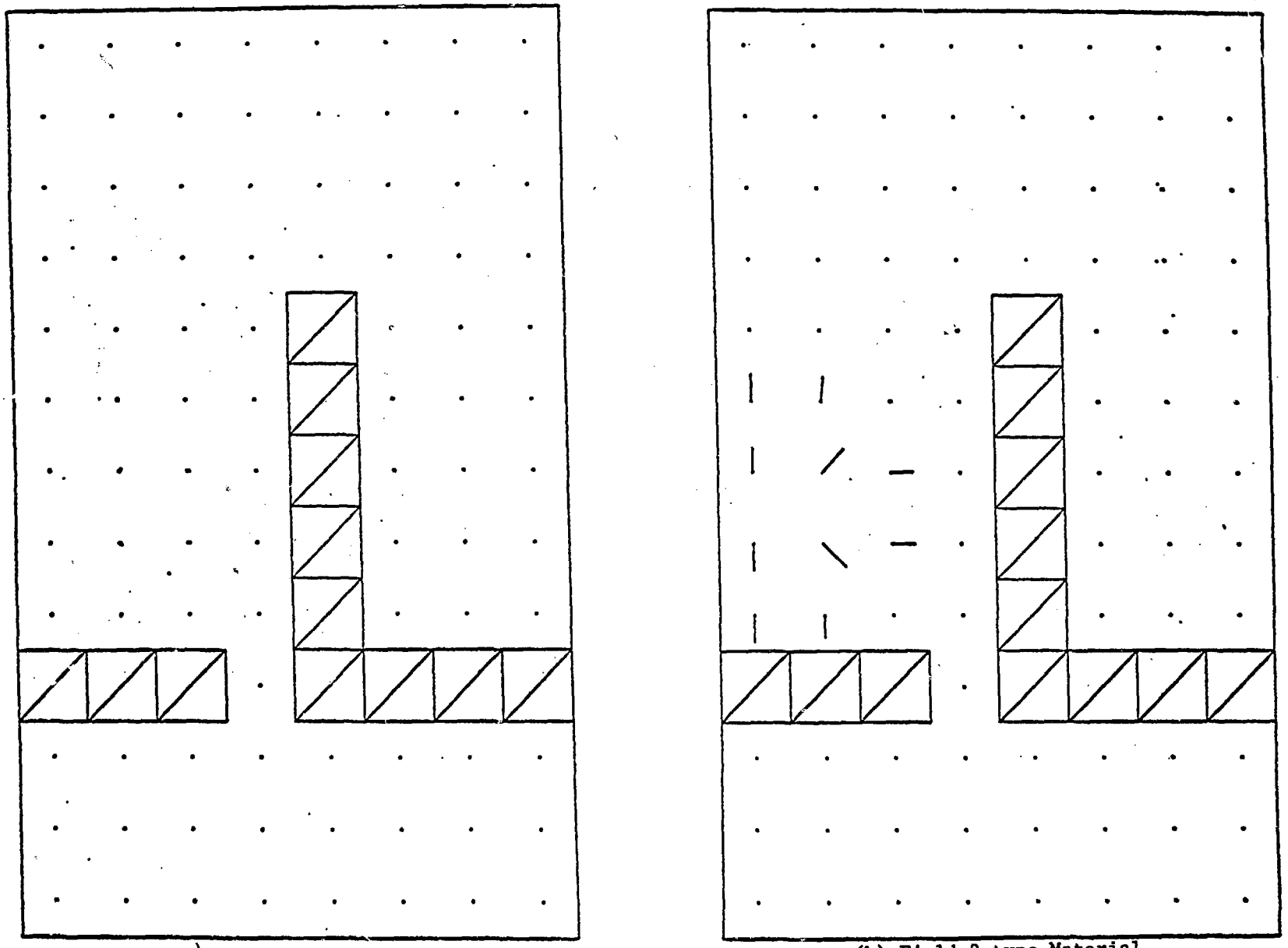

(a) Field-1 type Material

(b) Field 2 type Material

Fig. 2. Velocity-vector Plots at Beginning of Excursion (Example 1)

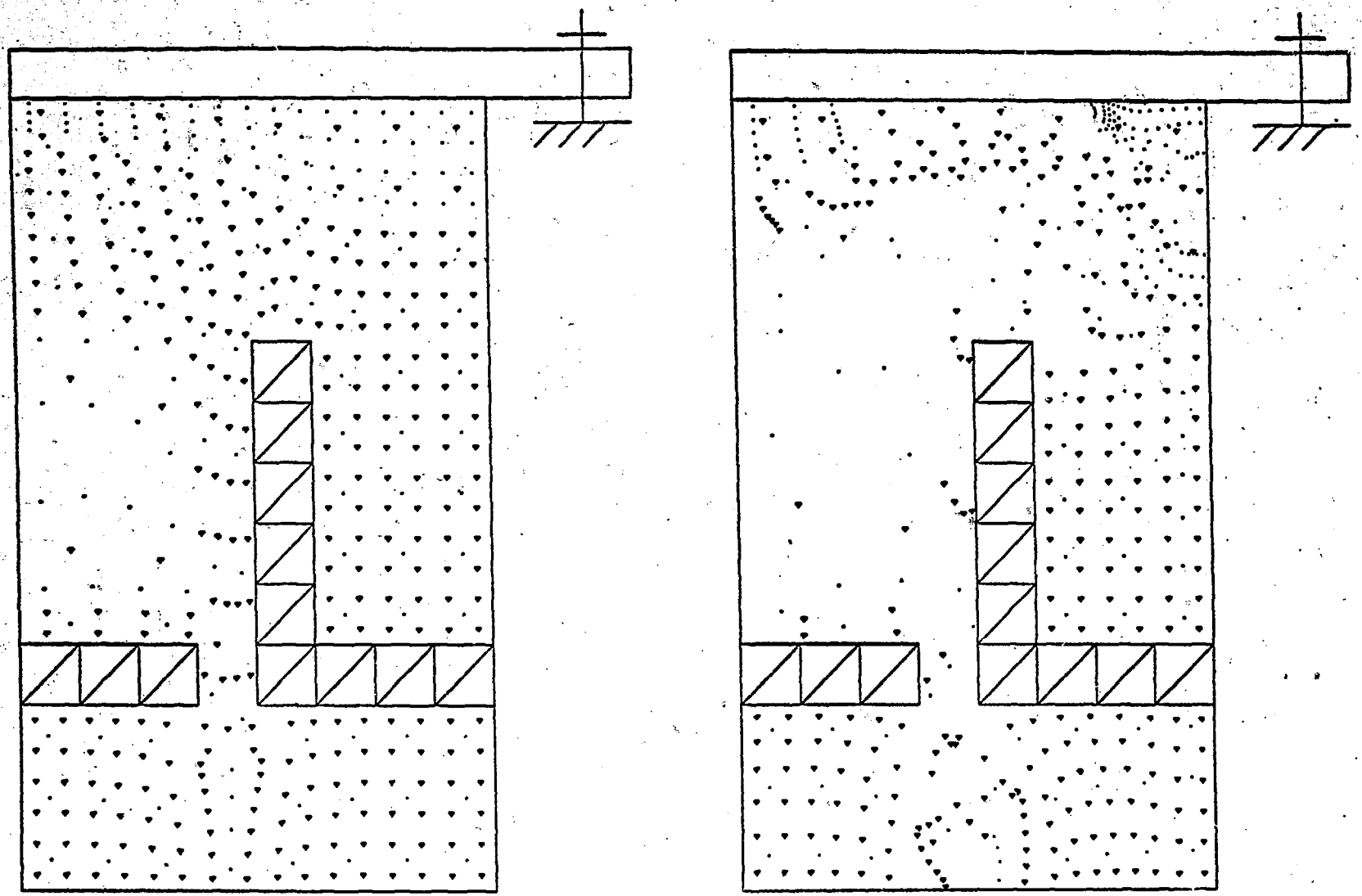

(a) t = 4.35 ms

(b) 14.35 ms

Fig. 3. Reactor Configurations at Two Distinct Instants (Example 1)

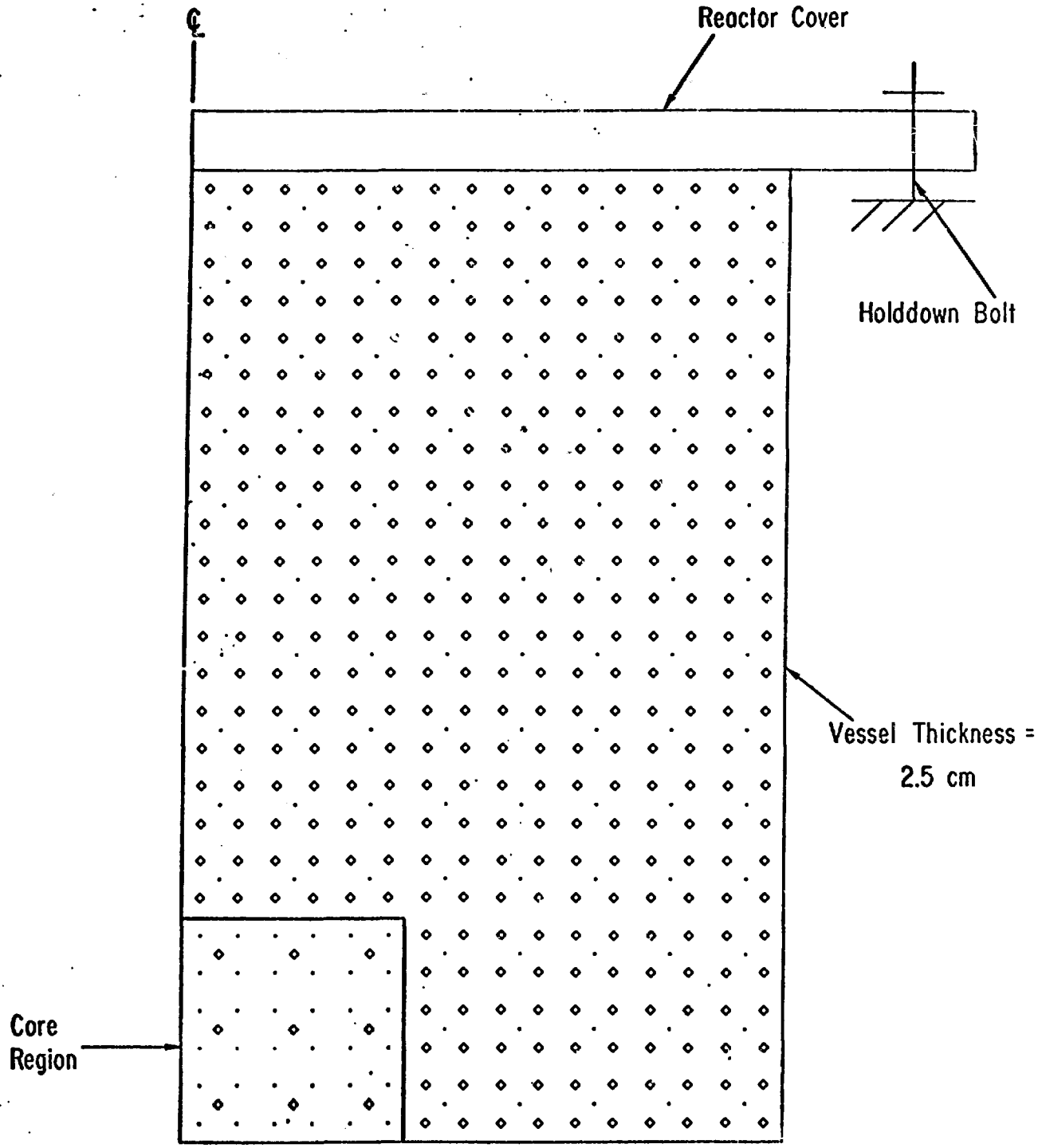

Fig. 4. Initial Configuration (Example 2)

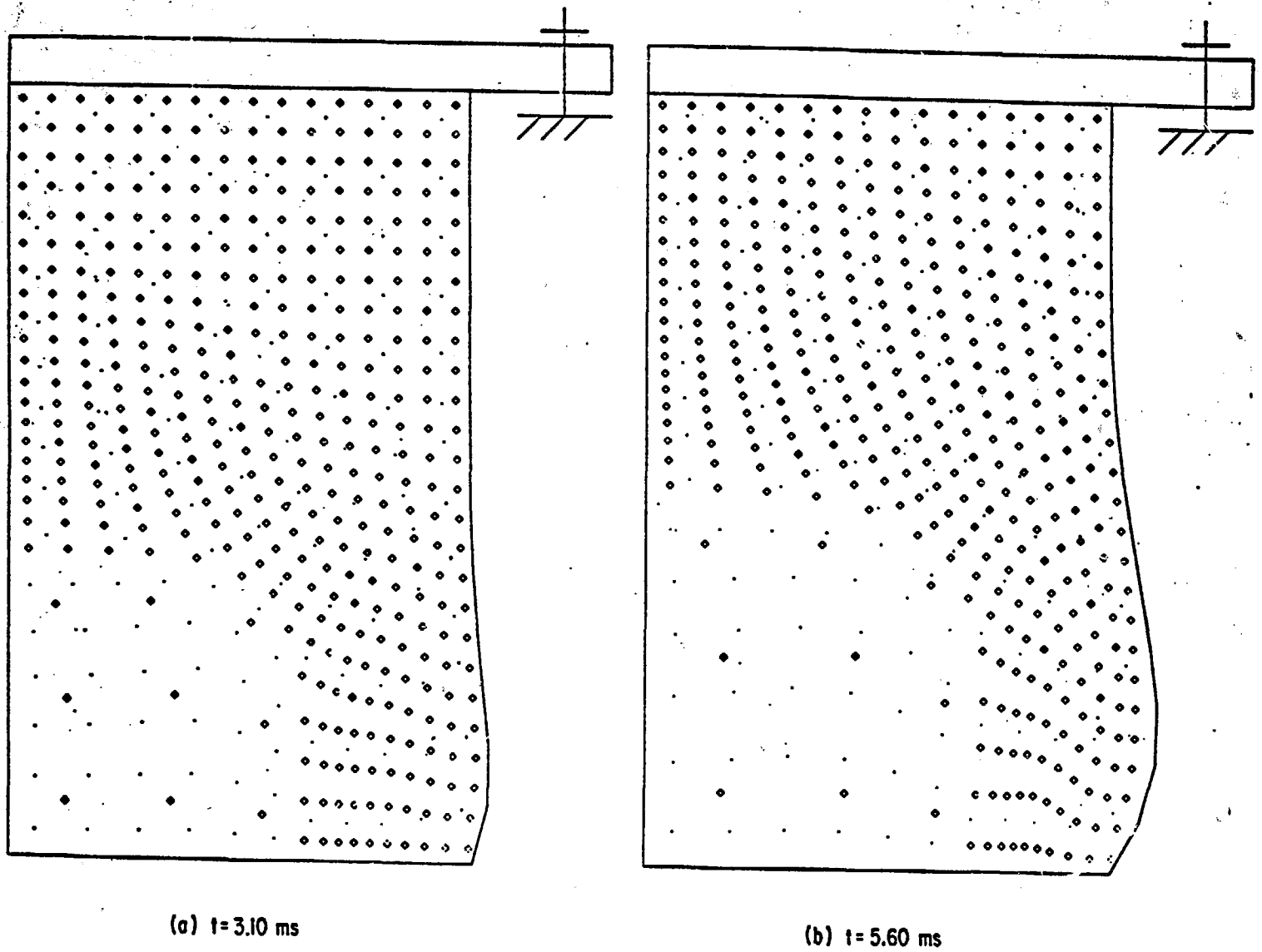

Fig. 5. Reactor Configurations at Two Distinct Instants (Example 2)